



An Investigation of the Requirements of an Airborne, Scanning, Polarimetric Phased Array Radar to Accurately Measure Hydrometeor Properties Near the Earth's Surface

Eric Loew and Jothiram Vivekanandan

Earth Observing Laboratory, National Center for Atmospheric Research, Boulder, CO 80301
ericloew@ucar.edu

Abstract

Accurately measuring the properties of weak weather echoes in the presence of strong ground clutter is a challenge for any ground-based scanning radar, but it is particularly difficult for scanning airborne radar whose beam routinely and directly intercepts the ground. If one further considers phased array radar which requires the use of pulse compression to compensate for the lack of available peak transmit power, the influence of the ability to accurately measure the properties of weather echoes near the surface is exacerbated not only by the antenna sidelobes, but also by range time sidelobes which are a side-effect of pulse compression. Normalized radar cross section (NRCS) of the Earth's surface has been characterized for land and water at various radar frequencies and grazing angles. NRCS data at C-band, will be examined in order to establish realistic expectations and requirements for Airborne Phased Array Radar (APAR) (Vivekanandan et al. 2014) for discerning weak weather echoes near the Earth's surface. The methodology used can be applied to analyze the requirements of other airborne scanning radars.

1. What is APAR?

APAR is a modular, dual-polarized, two-dimensional (2-D) electronically scanned C-band airborne phased array radar. It is currently in early development by the National Center for Atmospheric Research (NCAR). APAR will be capable of retrieving dynamic and microphysical characteristics of clouds and precipitation. The design of the NCAR APAR envisions it being flown on the National Science Foundation (NSF) NCAR C-130, operated by NCAR on behalf of NSF. There is the potential for APAR to be flown on other C-130 aircraft (e.g. U.S. Hurricane Hunters and similar international research aircraft) for hurricane reconnaissance and monitoring high impact weather. APAR is intended to replace NCAR's ELDORA/ASTRAIA (Electra Doppler Radar/Analyse Steroscopic Impulsions Aeroport)

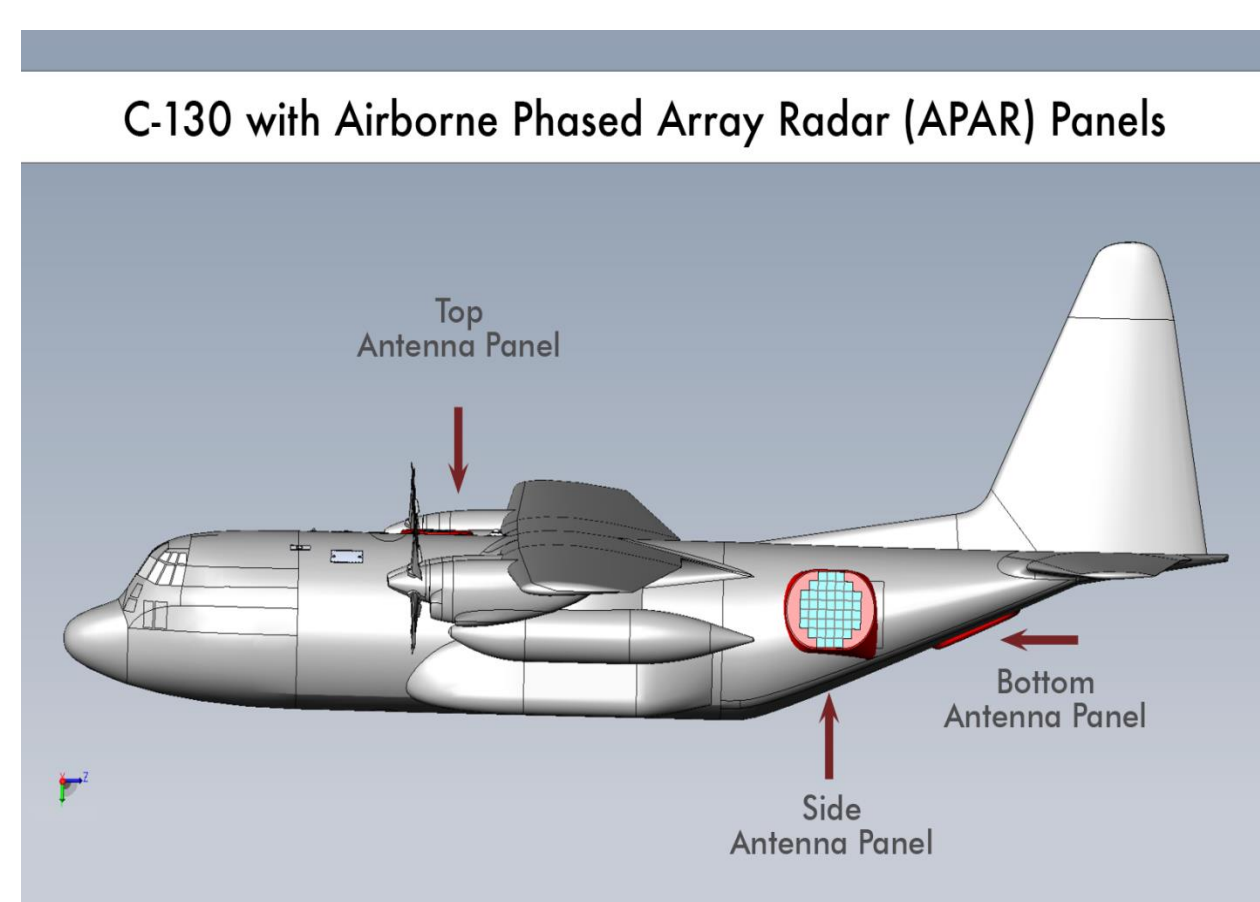


Figure 1 Notional drawing of APAR AESA antenna panel placement on the C130. There are two side panels on port and starboard of the fuselage aft of the rear personnel doors.

Parameter	Numeric value
Operating Frequency	C-band: 5.35 - 5.45 GHz (FAA requirement)
Antenna Aperture (maximum)	38" major and 35" in minor radius ellipse.
Maximum panel thickness	<= 9 inches
Maximum weight for each AESA assembly	<= 450 pounds
-3dB Beamwidth	< 2.2° (broadside on Tx)
Sensitivity	-11 dBZ at 10 km with 0 dB SNR
Reflectivity Variance	< 1 dB
Doppler Velocity Variance	< 1 m/s
Produce full polarimetric matrix	Z, V, W, Z _{DR} , LDR, ϕ _{DP} , ρ _{HV}
Calibrated Z _{DR} for particle shape and OPE	Z _{DR} <= 0.2 dB
Differentiate liquid and ice	LDR < -22 dB
Differentiate melting	LDR < -27 dB
Polarization Tx and Rx	H or V linear.

Table 1 Technical Specification of APAR

2. The Problem

For an airborne radar to accurately measure hydrometeor properties of weak weather echoes in the presence of strong clutter returns from the Earth's surface. To further compound the difficulty, Friedrich et al 2009 showed the signal to clutter ratios of Table 2 were required.

Parameter	Error	Signal/Clutter
Z _{cl}	< 1 dB	> 3 dB
Z _{DR}	< 0.2 dB	> 6 dB
ϕ _{DP}	< 3°	> 6 dB
ρ _{HV}	< 0.02	> 13.5 dB

Table 2 Signal to clutter ratios required to observe some hydrometeor properties within the error specified

3. Assumptions

For the simulations a circular phased array was used which had the characteristics shown in Table 3

Parameter	Value
Frequency	5.45 GHz
Aircraft Altitude	3000 m
Pulsewidth	1.0 μsec
Aperture Size	35" diameter
Transmit Power	9.7 kW
Element Gain	5.0 dB
Radar Constant	86.1 dB
Transmit Taper	15 dB Taylor Weighting
Receive Taper	30 dB Taylor Weighting
Peak Sidelobe Level	-49.6 dB
Integrated Sidelobe Level	-56.8 dB

Table 3 Simulated radar characteristics

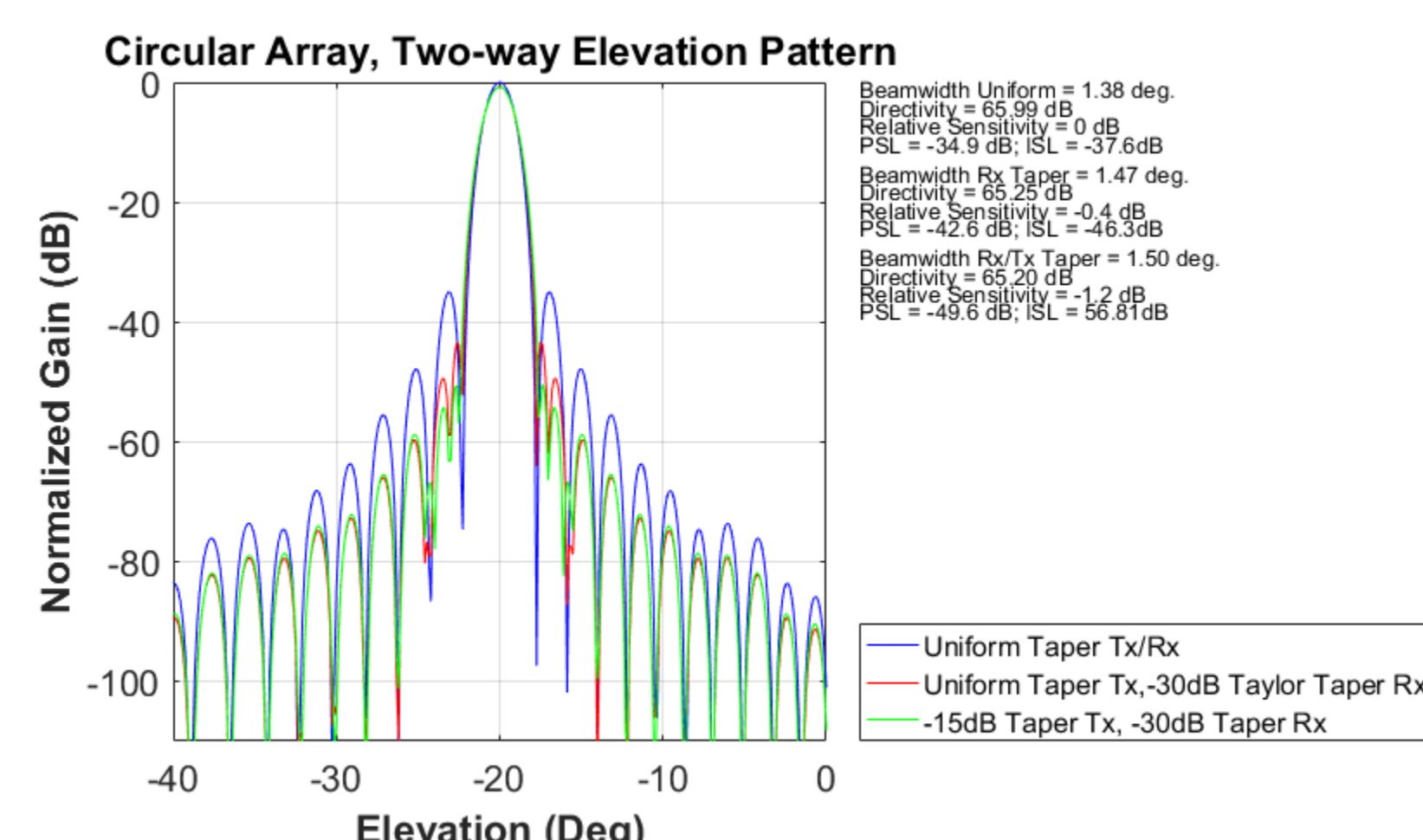


Figure 3 Normalized elevation pattern at -20° for circular array

4. Relation Between Surface And Volume Scattering Cross Sections

Airborne weather radar equation relates received power from a specified range and transmits power for a specified radar system parameters (Sekelsky, 2002) as

$$P_r = \frac{Z \sigma_0}{R^4 (h / \cos \theta)^2} \quad (1)$$

Where, $R_r = \frac{1024 \ln 2 \lambda^3 f_r 10^{34}}{P_r G_a^2 c^2 \tau \beta \phi |K|^2}$ (2) and the units for the variables are:

Z = radar reflectivity mm^6/m^3
P_r = power at the receiver (W),
P_t = peak transmit power (W),
c = the speed of light ($3 \times 10^8 \text{ ms}^{-1}$)
τ = RF pulse width (s)
G_a = antenna gain,
λ = radar signal wavelength (m),
β = antenna 3 dB beamwidth in horizontal and vertical in radians
K = radar dielectric constant for water
l_r = loss between the antenna and receiver port,
l_t = loss between the transmitter and the antenna port,
l_{atp} = one-way path-integrated atmospheric attenuation, along off-nadir angle θ
θ = radar beam incidence angle (radians)
σ₀ = normalized radar cross section (NRCS) for surface, and
h = altitude of the aircraft (m).

The basic form of a radar equation for surface scattering is (Kozu 1995):

$$P_r = \frac{P G_a^2 \lambda^3 \sigma_0 \beta \phi \cos(\theta)}{512 \ln 2 \pi^2 l_r l_t l_{atp}^2 h^2} \quad (3)$$

where all of the variables are defined above and l_{atp} one-way path-integrated atmospheric attenuation, along off-nadir angle θ.

The above surface and volume radar equations are used formulating radar reflectivity, Z in terms of NRCS (σ₀) as

$$Z = \sigma_0 \frac{2 \lambda^3 \cos(\theta)}{c \pi^2 |k|^2 l_{atp}^2} \quad (4)$$

It should be noted σ₀ is function of incidence angle whereas Z is independent of the incidence angle. For nadir pointing, figure 3a and 3b show Z and radar cross-section versus σ₀. When computing Z, atmospheric attenuation l_{atp} is ignored.

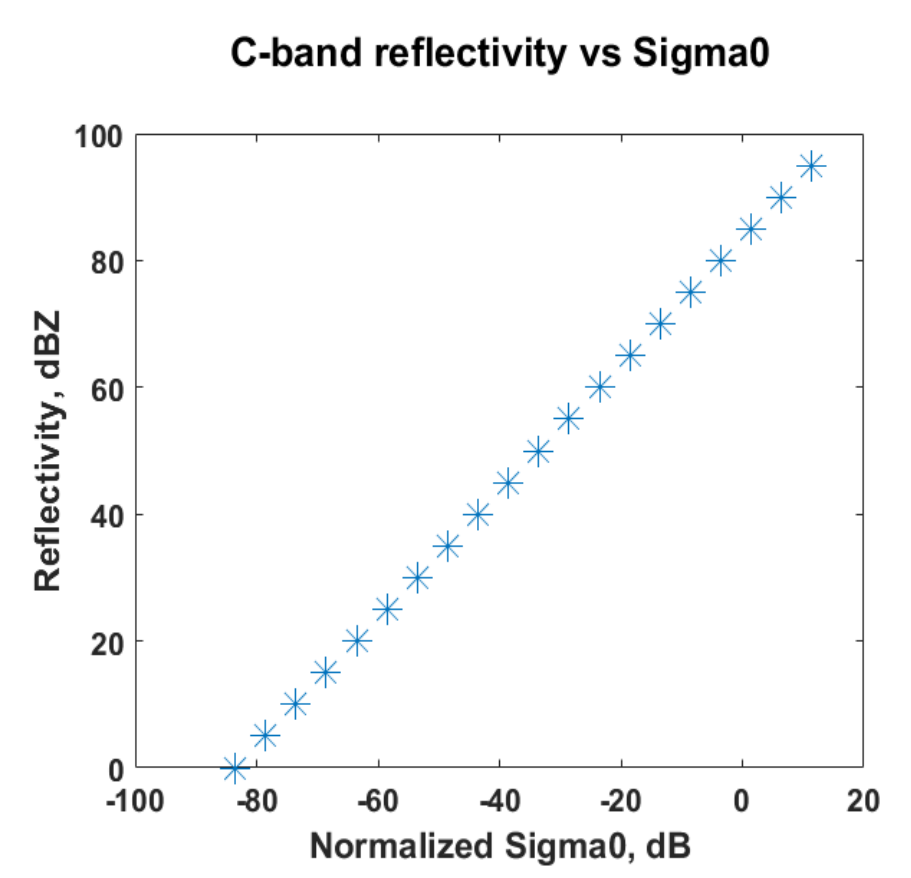


Figure 3a C-band weather radar reflectivity versus normalized radar cross-section of surface at nadir pointing direction

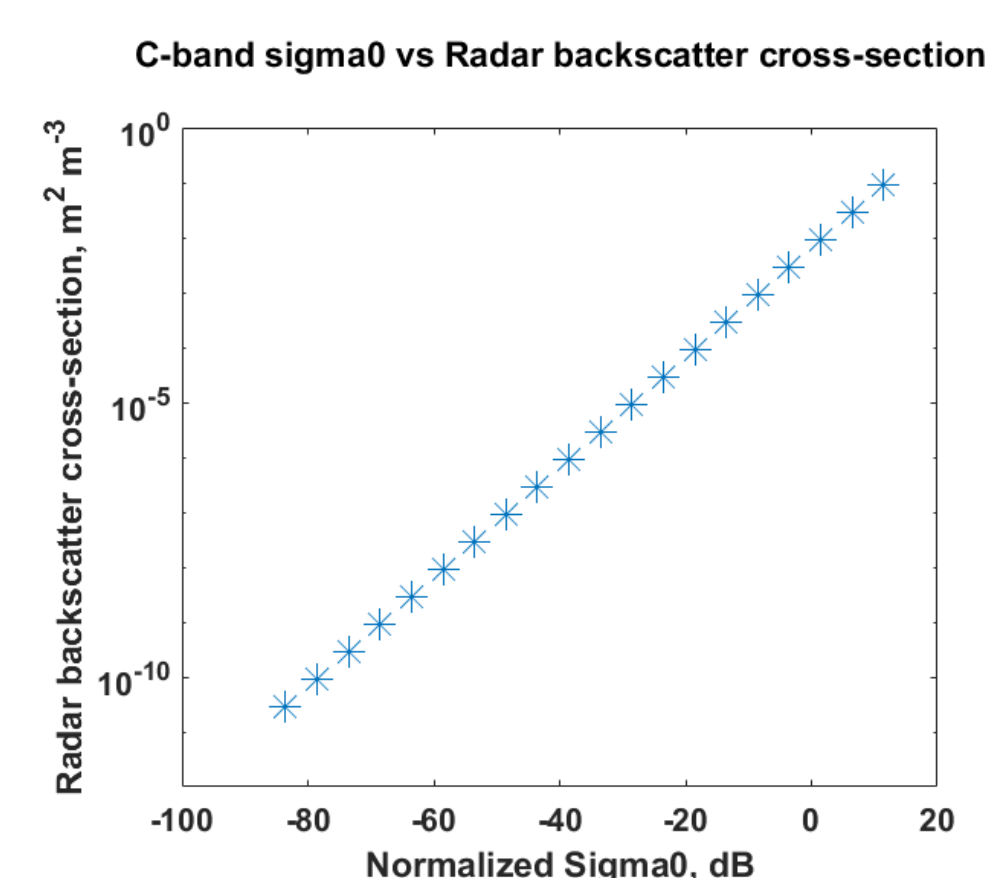


Figure 3b Normalized radar cross-section of surface at nadir pointing direction versus radar backscatter cross-sections of volume as in the case of weather radar

5. Land and Ocean Surface Scattering Measurements and Models

Since land and ocean scattering cross-sections are function of a range of physical variables, radar measurements of land and ocean varies over a wide range. In this research, a simpler version of land and ocean scattering models are used. These models describe average NRCS as a function of incidence angle. The following equation (Eaves and Reedy, 1987) describe NRCS of land in linear units,

$$\sigma_0 = A \left[\frac{e^{-q} + C^q \exp\left(-\frac{D}{1 + 0.15 \sigma_0}\right)} \right] \quad (5) \quad \text{Where } \theta = \text{radar beam incidence angle (radians)}$$

σ₀ = standard deviation of surface in the same units as wavelength
λ = radar signal wavelength
A, B, C and D are empirically derived constants as listed in Table 4

Constant	Soil/Sand	Grass	Tall Grass/ Crops	Trees	Urban
A	0.0096	0.015	0.015	0.0012	0.779
B	0.83	1.5	1.5	0.64	1.8
C	0.0013	0.012	0.012	0.002	0.015
D	2.3	0.0	0.0	0.0	0.0

Table 4 Constants A, B, C and D for given land types

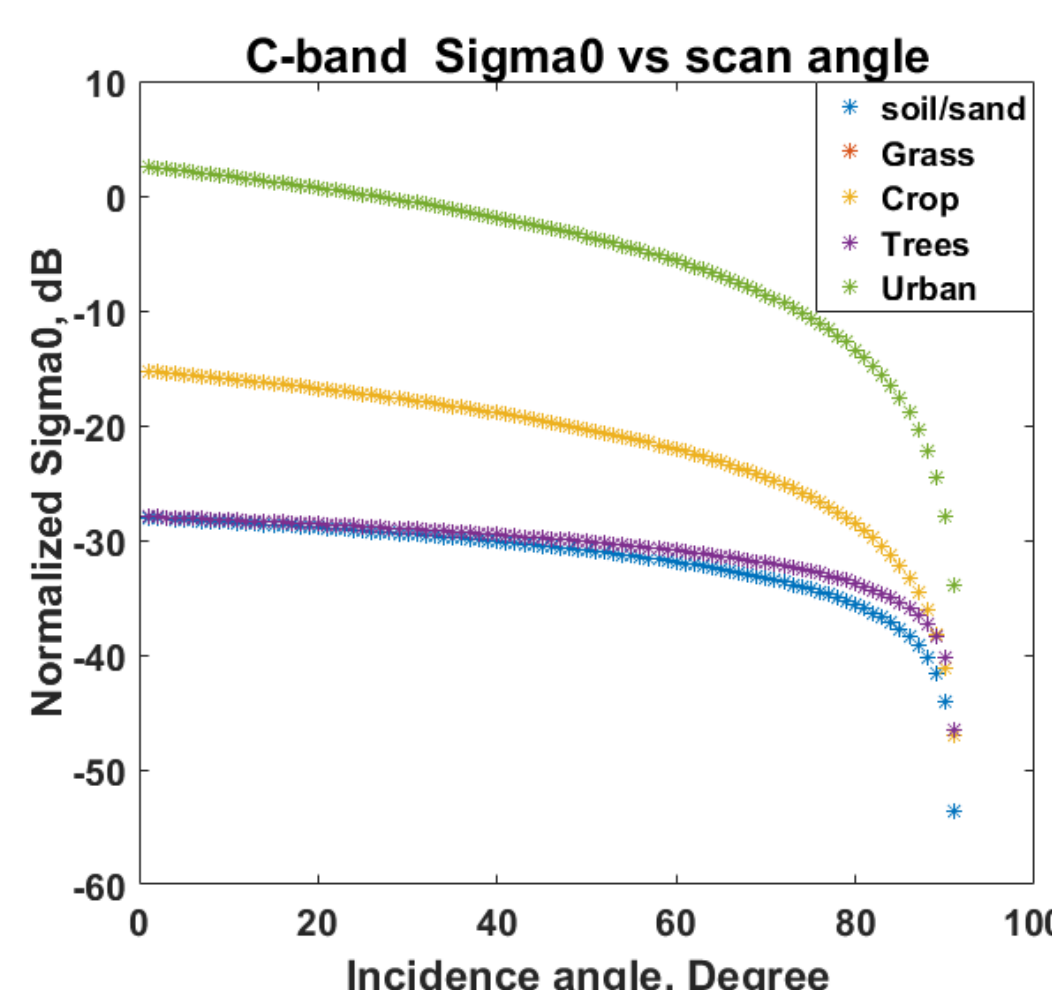


Figure 5 NRCS as a function of incidence angle for various land surfaces

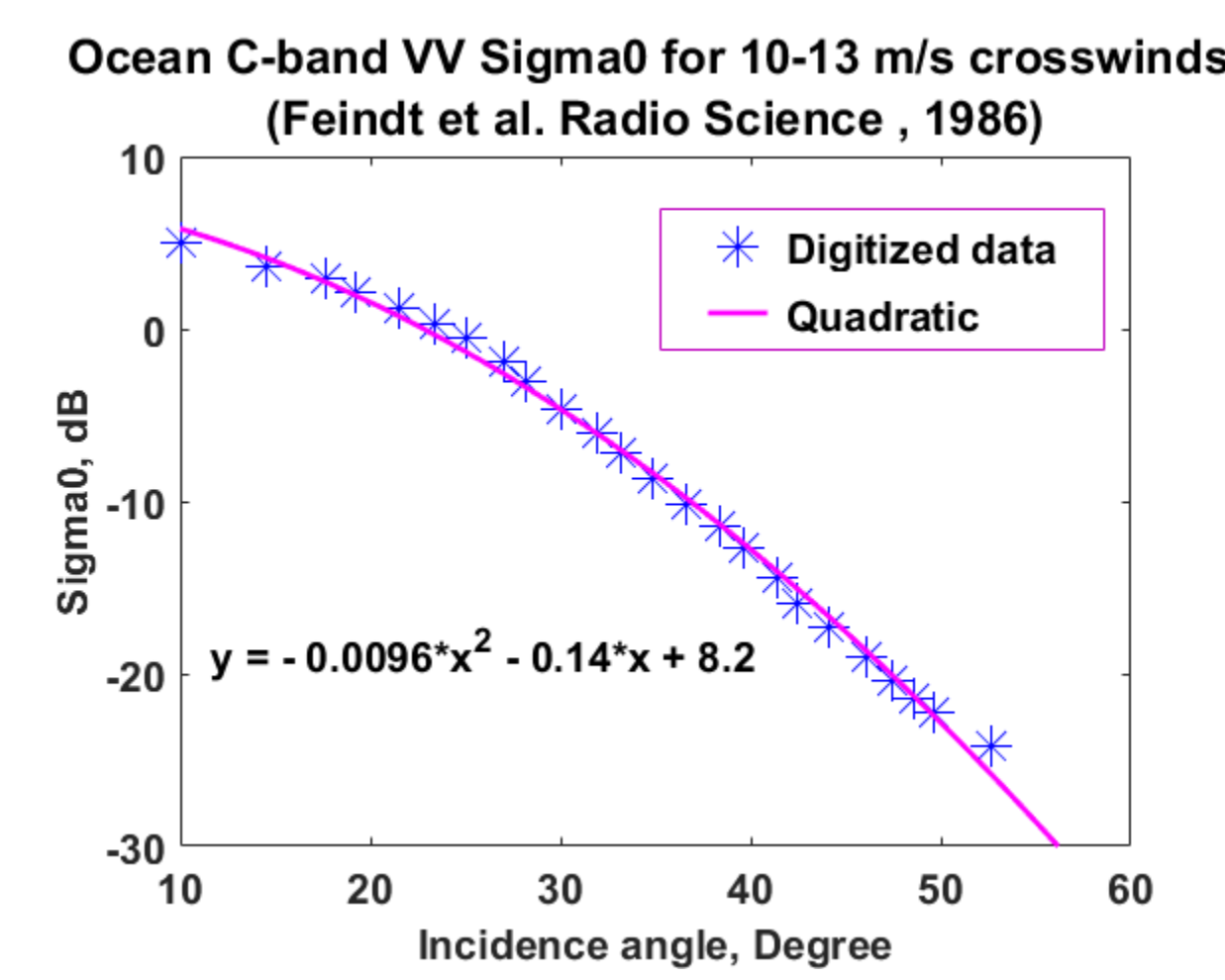


Figure 6 C-band Ocean NRCS as a function incidence angle for a mean sea-state

6. Calculating Surface Reflectivity Above Ground Level (AGL)

Method

- Calculate 3-D composite (Tx and Rx) antenna pattern in Cartesian coordinates (as shown in figures 9 and 10)
- Based on incidence angle and aircraft altitude, determine intersection of antenna pattern and surface which contribute to each range bin AGL
- Integrate over the lower half (in elevation) of this pattern; the upper half only affects those range bins beyond the surface
- Substitute integrated pattern: $\int_0^\pi \int_0^{2\pi} f^2(\theta, \phi) \sin \theta d\theta d\phi$ for $G_a^2 \pi \beta \phi / \ln 2$ in eq. (3), where $f^2(\theta, \phi)$ is the composite transmit, receive power gain antenna pattern
- Compute Z using eq. (1)

Surface Reflectivity (Ocean) vs. Incidence Angle

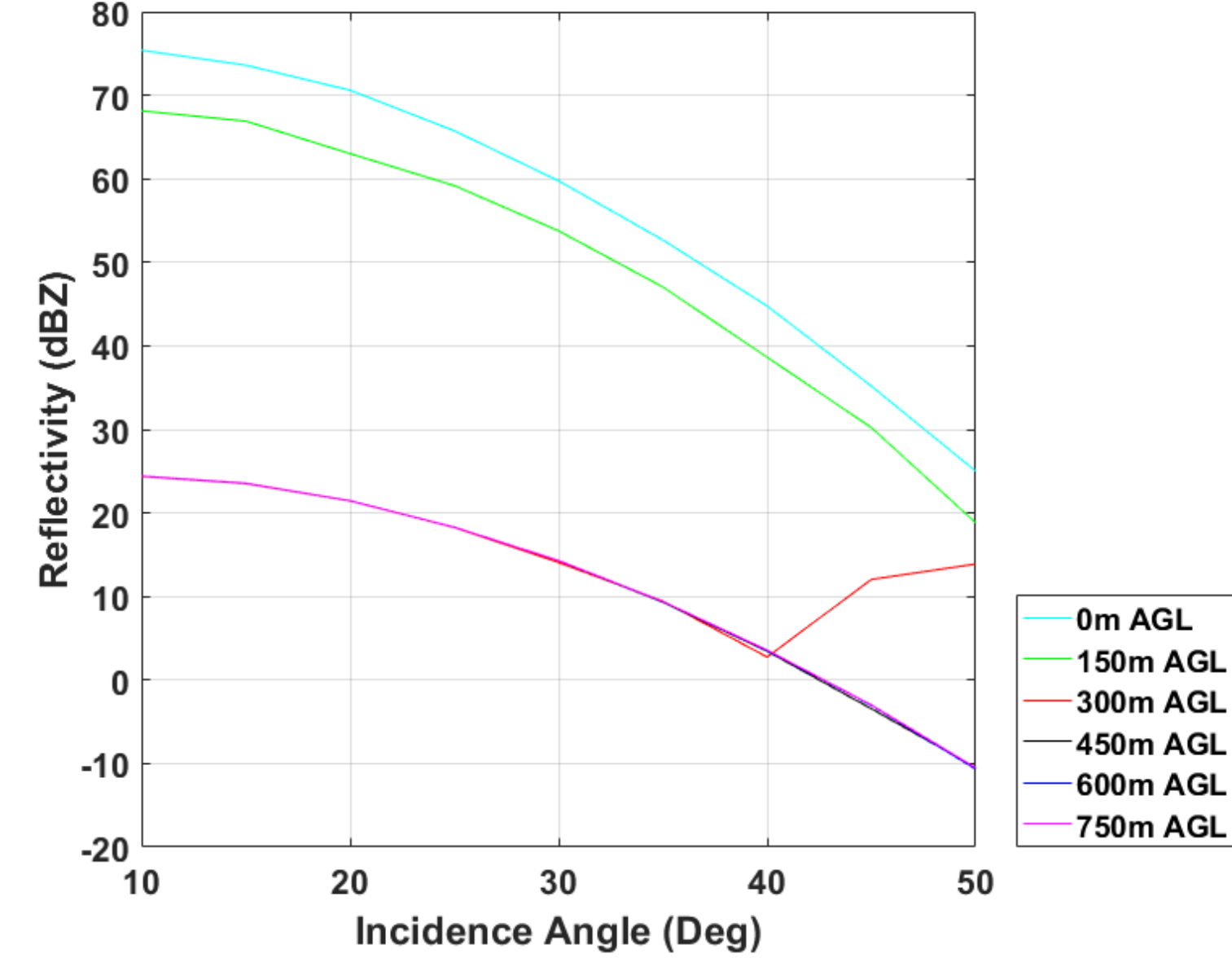


Figure 7 Reflectivity as a function of incidence angle over ocean for various ranges above the surface

Surface Reflectivity (Grass) vs. Incidence Angle

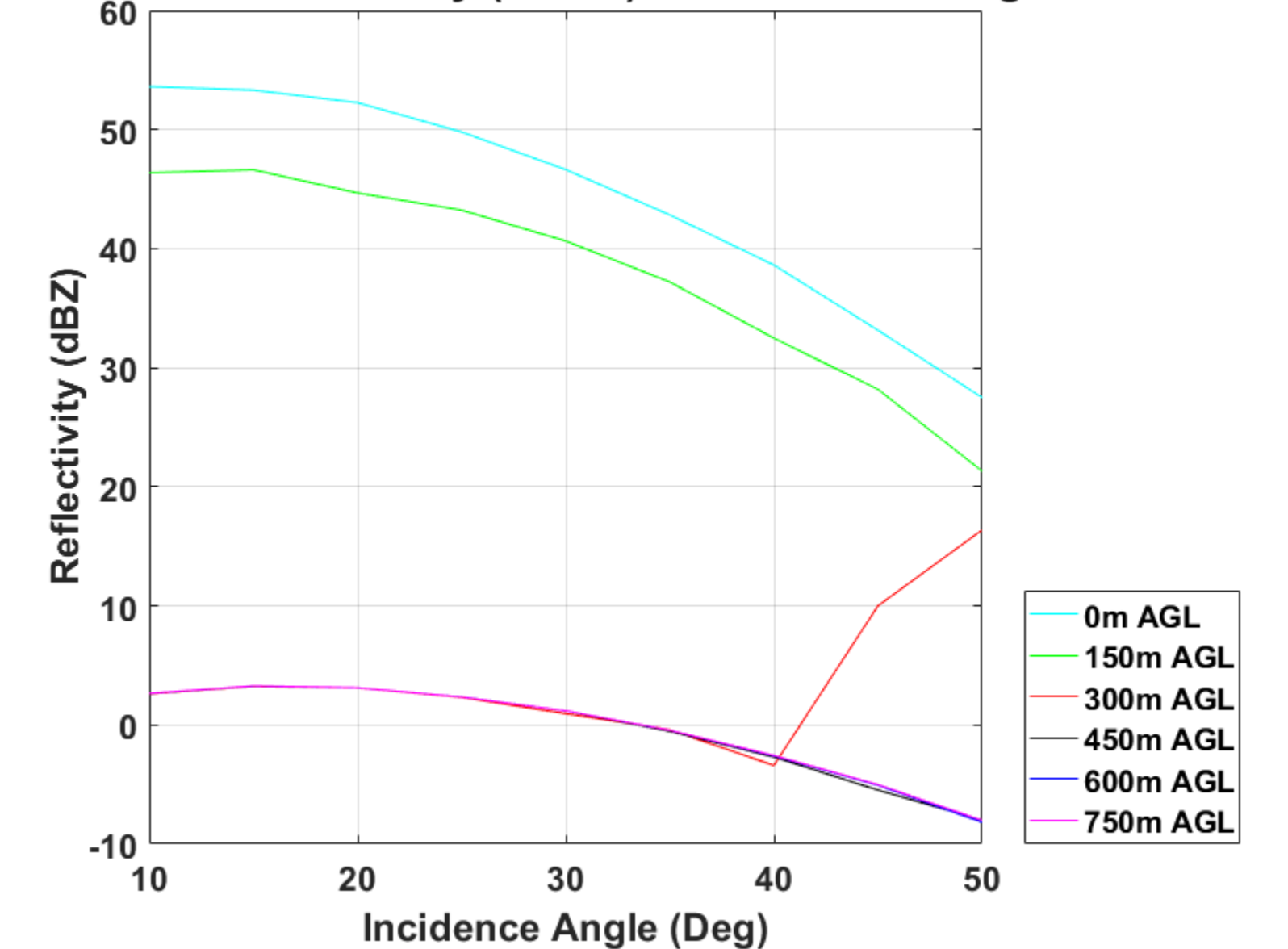


Figure 8 Reflectivity as a function of incidence angle over grass for various ranges above the surface

Composite Transmit Receive Antenna Pattern

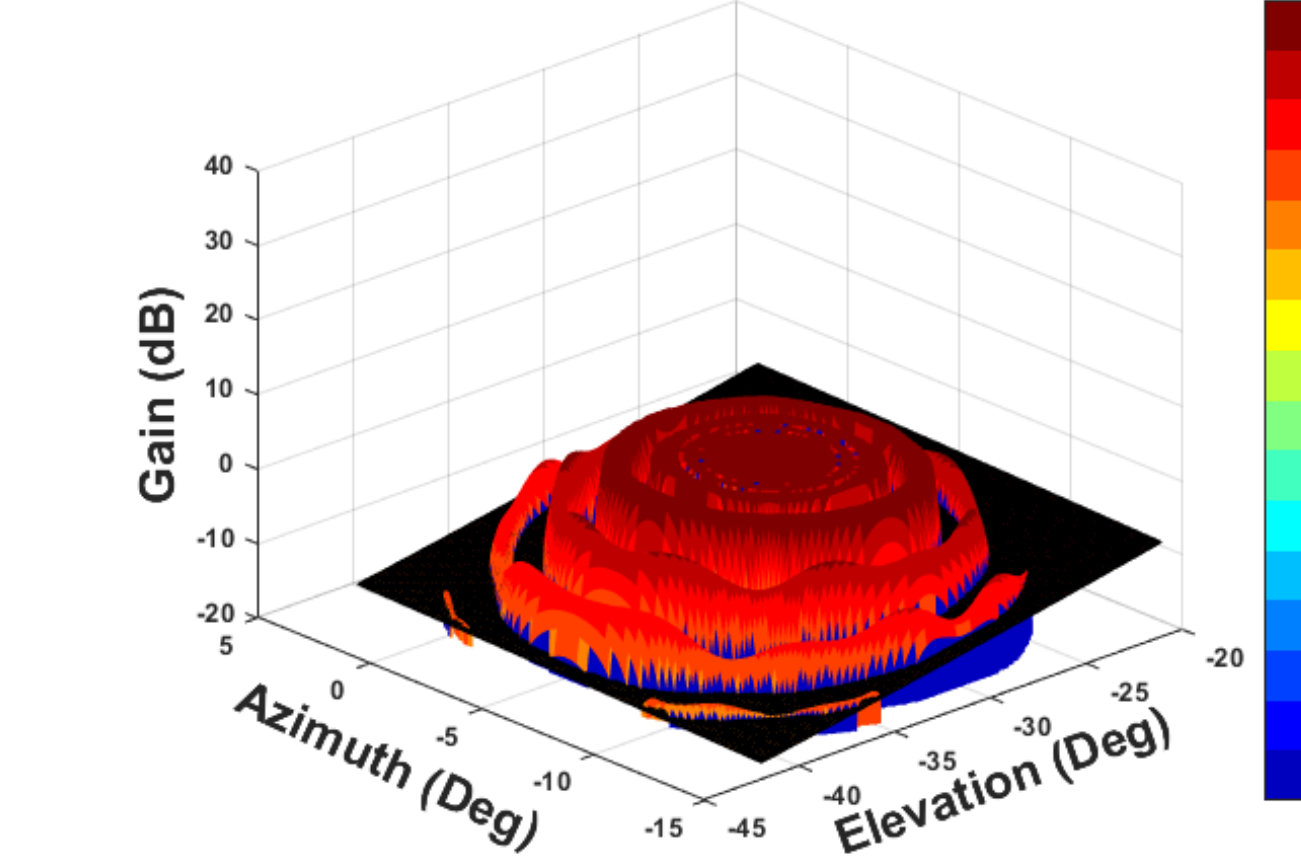


Figure 9 Composite transmit and receive antenna pattern for elevation of -30° (incidence angle of 30°) showing intersection with the surface, 300m AGL, represented by black plane

Composite Transmit Receive Antenna Pattern

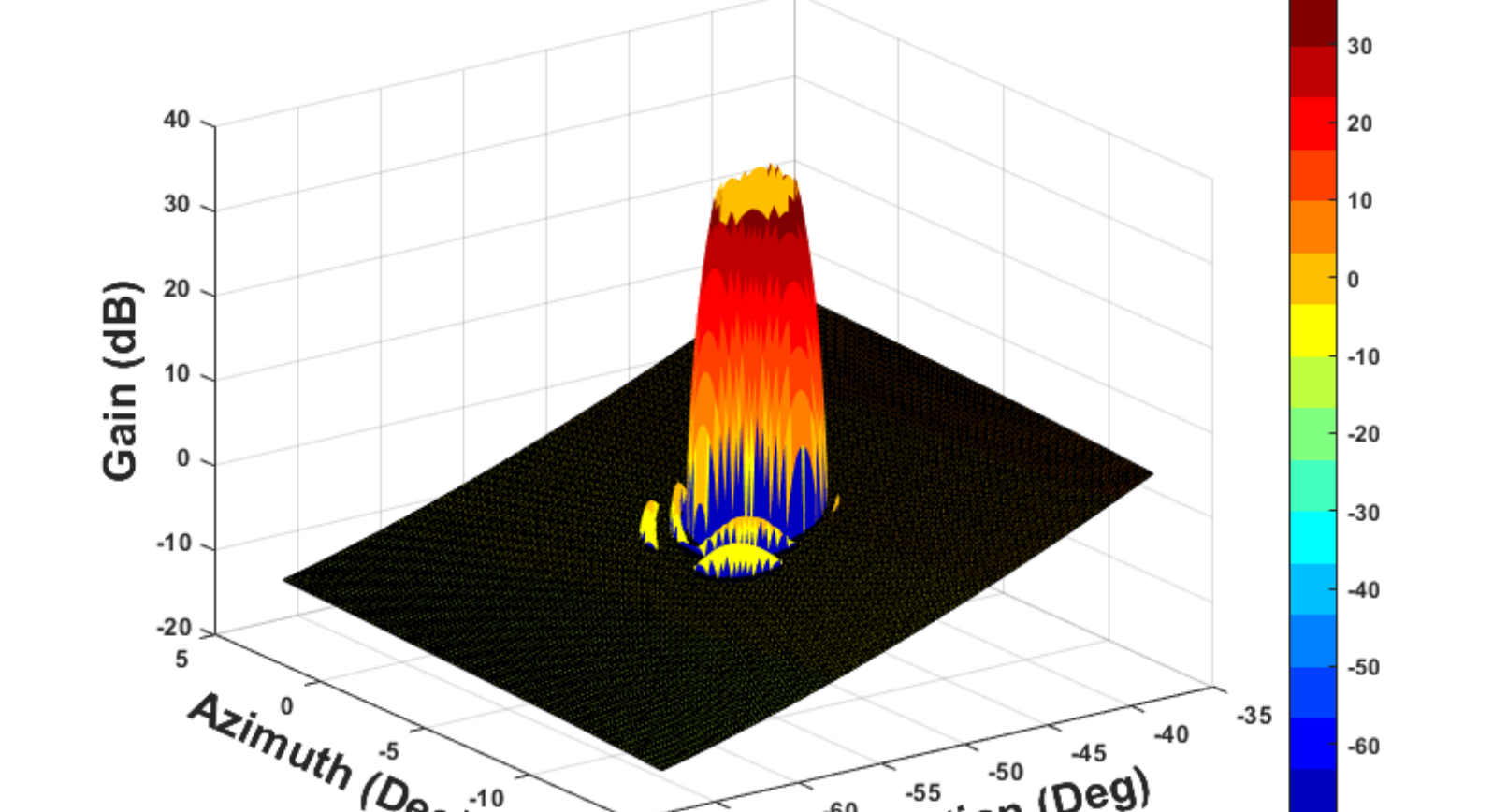


Figure 10 Composite transmit and receive antenna pattern for elevation of -50° (incidence angle of 50°) showing intersection with the surface, 300m AGL, represented by black plane

The increase in reflectivity at an AGL of 300m at incidence angles greater than 40 degrees can be explained by the amount of the antenna pattern being integrated at higher incidence angles. Figure 9 shows the composite pattern for 30 degree incidence, while figure 10 shows the same at 50 degrees. At 50 degrees the pattern intersection with the ground for 300m AGL still incorporates much of the main beam.

7 Summary and Future Work

- Based on our simulations and using the signal to clutter it is unlikely to detect weak weather (< 0 dBZ) for AGL's less than 450m
- Detection of weak weather over the ocean is particularly challenging as NRCS of ocean is higher than land (under most conditions)
- Investigate adaptive sidelobe cancellation to better reject surface clutter
- Expand simulations work to include:
 - varying the aircraft altitude
 - exploring antennas with different PSL and ISL
 - incorporating the effects of pulse compression

8 References

- Eaves, J. L., and E. K. Reedy, 1987: Principles of modern radar. Van Nostrand Reinhold Company, New York, pp 712.
- Feindt, F. V. Wisdemann, W. Alpers, and W. C. Keller, 1986: Airborne measurements of the ocean radar cross section at 5.3 GHz as a function of wind speed. Radio Sci., 21, 845-856.
- Friedrich, K., U. Germann and P. Tabary, 2009: Influence of ground clutter contamination on polarimetric radar parameters. J. Atmos. Ocean Tech., 26, 251-269.
- Kozu, T., 1995: A generalized surface echo radar equation for down-looking pencil beam radar. IEICE Trans. Commun., E78B, 1245-1248.
- Sekelsky, S., 2002: Near-field reflectivity and antenna boresight gain correction for millimeter-wave atmospheric radars. J. Atmos. Ocean Tech., 19, 468-477.
- Vivekanandan, J., W.-C. Lee, E. Loew, J. L. Salazar, V. Grubišić, J. Moore, and P. Tsai, 2014: The next generation airborne polarimetric Doppler weather radar. Geosci. Instrum. Method. Data Syst. Journal, 3, 111-126. doi:10.5194/gi-3-111-2014, 2014.

NCAR/EOL
3090 Center Green Dr.
Boulder, CO 80301
303.497.8801 ph
303.497.8770 fax
www.eol.ucar.edu

